

Local Rigidity in Sandpile Models

S. Ciliberti¹, G. Caldarelli¹, V. Loreto^{1,2} and L. Pietronero^{1,2}

¹INFM UdR Roma1 and “La Sapienza” University,

Physics Department, P.le A. Moro 5, 00185 Rome, Italy

² Center for Statistical Mechanics and Complexity (SMC), P.le A. Moro 5, 00185 Rome, Italy

We address the problem of the role of the concept of local rigidity in the family of sandpile systems. We define rigidity as the ratio between the critical energy and the amplitude of the external perturbation and we show, in the framework of the Dynamically Driven Renormalization Group (DDRG), that any finite value of the rigidity in a generalized sandpile model renormalizes to an infinite value at the fixed point, i.e. on a large scale. The fixed point value of the rigidity allows then for a non ambiguous distinction between sandpile-like systems and diffusive systems. Numerical simulations support our analytical results.

I. INTRODUCTION

The concept of Self Organized Criticality (SOC)^{1,2,3} has been proposed as a unifying theoretical framework to describe a vast class of driven systems that evolve “spontaneously” to a stationary state characterized by power law distributions of dissipation events. While originally SOC systems were associated to the absence of tuning parameters, it is now clear^{3,4} that most of the proposed systems show a critical behaviour only in the limit of an infinite separation of time scales, i.e. if some suitable parameter (e.g. the dissipation and the driving rate in sandpile models⁵, the temperature in some growth models⁶, etc.) is set to zero. These results suggested a new definition of SOC⁷ as the theory of dynamical processes that lead a system to the critical steady state if the critical value of the control parameter is zero.

The stabilizing effect of a threshold⁸ in the class of sandpile models is discussed by introducing a *local rigidity* defined as the ratio between the critical energy and the amplitude of the external perturbation, $r \equiv \varepsilon_c / \delta\varepsilon$. A finite rigidity allows the system to assume a large number of metastable configurations and this let the process show a power law distribution of avalanches. In⁸ it has been shown by means of numerical simulations that in the limit $r \rightarrow 0$ the system becomes a diffusive one characterized by only infinite avalanches. In this paper we show how, in the framework of the so-called Dynamically Driven Renormalization Group (DDRG)^{9,10}, a finite rigidity in the microscopic dynamics is crucial in order for the system to reach spontaneously a critical stationary state instead of a diffusive one. The basic idea is that at large scale the value of the rigidity does not depend on the microscopic value and that this “coarse grained” value allows for a non ambiguous distinction between a diffusive and a SOC system.

II. THE RENORMALIZATION OF THE RIGIDITY

In Sandpile Models we assign an integer variable (“energy”) ε_i on each site i of a d -dimensional hypercubic

lattice. At each time step an energy grain is added on a randomly chosen site, and then the system is allowed to relax according to a particular stability criterion depending on a fixed threshold (e.g. the energy, or the slope -defined as the difference between the energy of two nearest neighbours- exceeding a critical value). Infinite slow driving, i.e. an infinite separation of time scales, is built into the model: during the updating process the external input stops. The original BTW sandpile model¹ is a critical height model with $\varepsilon_c = 4$ and external input $\delta\varepsilon = 1$.

We consider a generalized sandpile model with critical height ε_c and external perturbation $\delta\varepsilon$ for the microscopic dynamics. If $\varepsilon_i > \varepsilon_c$ at time t then $\varepsilon_i = 0$ at time $t + 1$ and the q nearest neighbours of site i increase their value of ε_i/q . At the generic scale these quantities have the values $\varepsilon_c^{(k)}$ and $\delta\varepsilon^{(k)}$. The height of the stable sites is less than $\varepsilon_c^{(k)} - \delta\varepsilon^{(k)}$, for the critical sites the energy lies between $\varepsilon_c^{(k)} - \delta\varepsilon^{(k)}$ and $\varepsilon_c^{(k)}$ while for unstable sites it is larger than $\varepsilon_c^{(k)}$. We study the behaviour of $\varepsilon_c^{(k)}$ and $\delta\varepsilon^{(k)}$ under the renormalization flow of the DDRG which could be formally written as:

$$\varepsilon_c^{(k+1)} = f\left(\varepsilon_c^{(k)}, \delta\varepsilon^{(k)}; \rho^{(k)}, \mathbf{P}^{(k)}\right) \quad (1)$$

$$\delta\varepsilon^{(k+1)} = g\left(\varepsilon_c^{(k)}, \delta\varepsilon^{(k)}; \rho^{(k)}, \mathbf{P}^{(k)}\right)$$

where $\rho^{(k)}$ (density of critical sites) and $\mathbf{P}^{(k)} \equiv (p_1^{(k)}, p_2^{(k)}, p_3^{(k)}, p_4^{(k)})$ (p_n is the probability that in a toppling the energy is distributed exactly to n nearest neighbours) are the parameters characterizing the state at the generic scale k . In principle we have to couple these two equations to those that determine the renormalization of $\rho^{(k)}$ and $\mathbf{P}^{(k)}$; for sake of simplicity, having extended the parameters space, we assume that the flow of the new parameters is orthogonal to the space defined by the old ones. We then accordingly fix $\rho^{(k)}$ and $\mathbf{P}^{(k)}$ to their fixed point values ρ^* and \mathbf{P}^* as computed in ref.[9]. Their values are $\rho^* = 0.468$ and $\mathbf{P}^* = (0.240, 0.442, 0.261, 0.057)$. The validity of this approximation will be checked by numerical simulations. Our transformation will have the

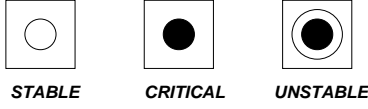
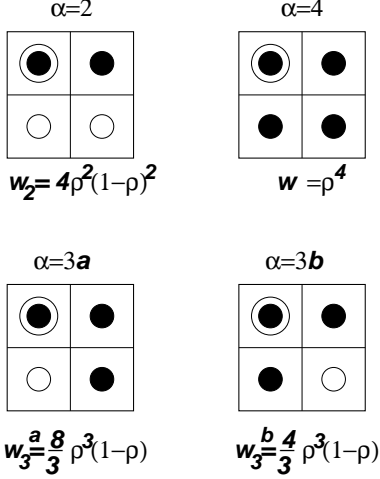


FIG. 1: Critical, stable and unstable sites.

FIG. 2: The α configurations with relative statistical weights.

form:

$$\begin{aligned}\varepsilon_c^{(k+1)} &= f\left(\varepsilon_c^{(k)}, \delta\varepsilon^{(k)}; \rho^*, \mathbf{P}^*\right) \\ \delta\varepsilon^{(k+1)} &= g\left(\varepsilon_c^{(k)}, \delta\varepsilon^{(k)}; \rho^*, \mathbf{P}^*\right)\end{aligned}\quad (2)$$

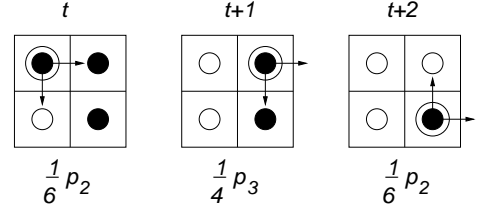
The symbols used are shown in Fig. 1 and 2.

Let us consider now a single path as an example of the transformation we want to obtain. We have a 2×2 cell characterized by a label α specifying the number of critical sites. The $\alpha = 1$ configuration is not considered because of a *spanning rule* that imposes the exclusion of those processes that do not relax within the cell before they transfer energy outside. Every configuration α has a mean height $\langle\varepsilon_\alpha\rangle$ that we calculate in the next section. One of the possible evolution from the configuration $\alpha = 3a$ state is shown in Fig. 3.

This means that at the scale $k + 1$ the mean height of the considered cell is critical with probability

$$\pi \equiv w_{\alpha=3}^{(a)}(\rho^*) \cdot \frac{1}{6} p_2^* \cdot \frac{1}{4} p_3^* \cdot \frac{1}{6} p_2^* \quad (3)$$

As a matter of fact, the cell has a probability π to be a critical site at the scale $k + 1$. The complete renormalization flow is therefore a sum over all the configuration and over all the possible paths of terms like $\pi \cdot \langle\varepsilon_{\alpha=3}^{(k)}\rangle$. In the same process we observe that with probability π the quantity given outside of the cell, $\delta\varepsilon^{(k+1)}$, is $3/2 \cdot \delta\varepsilon^{(k)}$. 3 flows of energy $\delta\varepsilon^{(k)}$ are lost outside the cell passing

FIG. 3: One of the possible time evolutions starting from an $\alpha = 3$ configuration and transferring energy outside of the cell; for every step the relative probability is indicated.

through 2 sides. It means that for this transformation we have to distinguish paths transferring the same energy through a different number of sides. The general transformations are

$$\begin{aligned}\varepsilon_c^{(k+1)} &= \sum_{\alpha} w_{\alpha}(\rho^*) \left[\langle\varepsilon_{\alpha}^{(k)}\rangle \cdot \sum_i P_{i,\alpha}(\mathbf{P}^*) \right] \\ \delta\varepsilon^{(k+1)} &= \sum_{\alpha} w_{\alpha}(\rho^*) \left[\sum_i P_{i,\alpha}^{n,m}(\mathbf{P}^*) \frac{n}{m} \cdot \delta\varepsilon^{(k)} \right]\end{aligned}\quad (4)$$

where $P_{i,\alpha}$ are the probabilities relative to time evolutions that transfer energy outside of the cell, while $P_{i,\alpha}^{n,m}$ refers to a process that let n quanta going through m sides.

We compute now the average energy per site in all the configurations. We generalize the simple mean field argument described in ref.[11], making the simpler non trivial assumption for the probability distribution of the energy: $P(\varepsilon) = a + b\varepsilon$. The normalization

$$\int_0^{\varepsilon_c} d\varepsilon P(\varepsilon) = 1 \quad (5)$$

implies that $b = 2(1 - a\varepsilon_c)/\varepsilon_c^2$.

The average energy is then expressed in term of the parameter a :

$$\langle\varepsilon\rangle \equiv \int_0^{\varepsilon_c} d\varepsilon \varepsilon P(\varepsilon) = \frac{2}{3} \varepsilon_c - \frac{1}{6} a \varepsilon_c^2. \quad (6)$$

Following ref.[11] we find that $a \simeq 0.277/\varepsilon_c$. The average energy of stable and critical sites is then:

$$\begin{aligned}\langle\varepsilon\rangle_{stable} &\equiv \frac{\int_0^{\varepsilon_c - \delta\varepsilon} d\varepsilon \varepsilon P(\varepsilon)}{\int_0^{\varepsilon_c - \delta\varepsilon} d\varepsilon P(\varepsilon)} = \frac{\int_0^{\varepsilon_c - \delta\varepsilon} d\varepsilon \left(a\varepsilon + \frac{2}{\varepsilon_c^2} \varepsilon^2 (1 - a\varepsilon_c) \right)}{\int_0^{\varepsilon_c - \delta\varepsilon} d\varepsilon \left(a + \frac{2}{\varepsilon_c^2} \varepsilon (1 - a\varepsilon_c) \right)} \\ &= \frac{\frac{2}{3} - \frac{1}{6} a \varepsilon_c - \frac{\delta\varepsilon}{\varepsilon_c} \left(\frac{4}{3} - \frac{5}{6} a \varepsilon_c \right) + O(\delta\varepsilon)^2}{\frac{1}{\varepsilon_c} \left[1 - \frac{\delta\varepsilon}{\varepsilon_c} (1 - a\varepsilon_c) \right]} \\ &= \langle\varepsilon\rangle - \frac{2}{3} \delta\varepsilon \left(1 - \frac{1}{4} a^2 \varepsilon_c^2 \right) + O(\delta\varepsilon)^2\end{aligned}\quad (7)$$

$$\begin{aligned}
\langle \varepsilon \rangle_{critical} &\equiv \frac{\int_{\varepsilon_c - \delta\varepsilon}^{\varepsilon_c} d\varepsilon \varepsilon P(\varepsilon)}{\int_{\varepsilon_c - \delta\varepsilon}^{\varepsilon_c} d\varepsilon P(\varepsilon)} = \frac{\int_{\varepsilon_c - \delta\varepsilon}^{\varepsilon_c} d\varepsilon \left(a\varepsilon + \frac{2}{\varepsilon_c^2} \varepsilon^2 (1 - a\varepsilon_c) \right)}{\int_{\varepsilon_c - \delta\varepsilon}^{\varepsilon_c} d\varepsilon \left(a + \frac{2}{\varepsilon_c^2} \varepsilon (1 - a\varepsilon_c) \right)} \\
&= \frac{\varepsilon_c (2 - a\varepsilon_c) - \delta\varepsilon \left(2 - \frac{7}{2} a\varepsilon_c \right)}{(2 - a\varepsilon_c) \left[1 - \frac{\delta\varepsilon}{\varepsilon_c} \frac{1 - a\varepsilon_c}{2 - a\varepsilon_c} \right]} \\
&= \varepsilon_c - \delta\varepsilon \frac{1 - \frac{5}{2} a\varepsilon_c}{2 - a\varepsilon_c} + O(\delta\varepsilon)^2
\end{aligned} \tag{8}$$

If we put $a = 0.277/\varepsilon_c$ in these expressions we obtain

$$\langle \varepsilon \rangle_{stable} = 0.6205 \varepsilon_c - 0.539 \delta\varepsilon \tag{9}$$

$$\langle \varepsilon \rangle_{critical} = \varepsilon_c - 0.1785 \delta\varepsilon \tag{10}$$

The average energy per site for different configurations can now be calculated as

$$\langle \varepsilon_{\alpha=2} \rangle = \frac{1}{4} [2 \langle \varepsilon \rangle_{critical} + 2 \langle \varepsilon \rangle_{stable}] = 0.810 \varepsilon_c - 0.359 \delta\varepsilon \tag{11}$$

$$\langle \varepsilon_{\alpha=3} \rangle = \frac{1}{4} [3 \langle \varepsilon \rangle_{critical} + \langle \varepsilon \rangle_{stable}] = 0.905 \varepsilon_c - 0.269 \delta\varepsilon \tag{12}$$

$$\langle \varepsilon_{\alpha=4} \rangle = \langle \varepsilon \rangle_{critical} = \varepsilon_c - 0.1785 \delta\varepsilon \tag{13}$$

Equations for the renormalization flow have the form

$$\begin{cases} \varepsilon_c^{(k+1)} = a \varepsilon_c^{(k)} - b \delta\varepsilon^{(k)} \\ \delta\varepsilon^{(k+1)} = c \delta\varepsilon^{(k)} \end{cases} \tag{14}$$

where the coefficients a, b and c obviously depend on the fixed point parameters. If we divide the two equations, recalling the definition of the rigidity, we obtain

$$r^{(k+1)} = \frac{a}{c} r^{(k)} - \frac{b}{c}. \tag{15}$$

The fixed point of the rigidity corresponds to setting $r^{(k+1)} = r^{(k)} = r^*$:

$$r^* = \frac{b}{a - c}. \tag{16}$$

Next section deals with the calculation of the coefficients a, b and c .

III. ANALYTICAL RESULTS

To calculate the coefficients a, b and c we have to distinguish between 4 different kind of configurations, each one with the relative weights $w_\alpha(\rho)$ as calculated in ref.[9].

- $\alpha = 2$

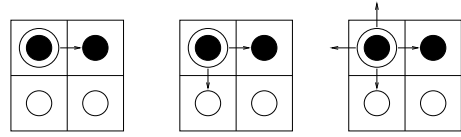


FIG. 4: Time t : the probability relative to the paths in figure is $\frac{1}{4}p_1 + \frac{1}{2}p_2 + \frac{3}{4}p_3 + p_4$.

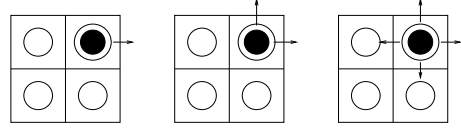


FIG. 5: Time $t+1$: the probability associated with the paths in figure is $\frac{1}{2}p_1 + \frac{5}{8}p_2 + p_3 + p_4$.

We consider at time t one of the toppling represented in Fig. 4 and possible developments at time $t+1$ in Fig. 5.

All the paths described transfer energy outside the cell, the associated probabilities are given in captions. Configuration $\alpha = 2$ then contributes with the term

$$\begin{aligned}
\varepsilon_c^{(k+1)} &= w_{\alpha=2}(\rho) \cdot \langle \varepsilon_{\alpha=2}^{(k)} \rangle \cdot \left(\frac{1}{4}p_1 + \frac{1}{2}p_2 + \frac{3}{4}p_3 + p_4 \right) \times \\
&\quad \times \left(\frac{1}{2}p_1 + \frac{5}{6}p_2 + p_3 + p_4 \right) + \dots \tag{17}
\end{aligned}$$

to the renormalization of the critical energy. Moreover, each of the described paths transfer only a quantum of energy outside of the cell, so

$$\begin{aligned}
\frac{\delta\varepsilon^{(k+1)}}{\delta\varepsilon^{(k)}} &= w_{\alpha=2}(\rho) \cdot \left(\frac{1}{4}p_1 + \frac{1}{2}p_2 + \frac{3}{4}p_3 + p_4 \right) \times \\
&\quad \times \left(\frac{1}{2}p_1 + \frac{5}{6}p_2 + p_3 + p_4 \right) + \dots \tag{18}
\end{aligned}$$

The details of the calculations regarding paths from configurations $\alpha = 3a, 3b$ and 4 are given in the appendix.

The final result is obtained by summing all these contributes that we have explicitly calculated with the respective weights. We find for the coefficients the following values:

$$a = 0.26 \pm 0.03 \quad b = 0.10 \pm 0.02 \quad c = 0.26 \pm 0.05 \tag{19}$$

We finally obtain that a and c are equal, even though the errors associated are relatively large. These errors are related to the parameters of the fixed point. Since they have only 3 significant digits, that results an error of order 10^{-3} .

We then find that the fixed point spontaneously reached by a sandpile model corresponds to an infinite value of the rigidity. It means that every finite value for

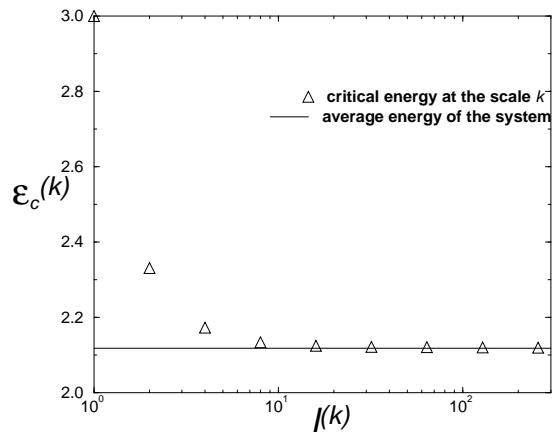


FIG. 6: The behaviour of the critical energy $\varepsilon_c^{(k)}$ at the scale k in the BTW sandpile model.

the microscopic dynamics renormalizes to an infinite one on a large scale.

The difference with a diffusive system is now clear: in the diffusive case a particle added from outside can always go out of the system from the boundaries, while in a SOC system this is avoided by the value of the rigidity as bigger as observed from a large scale.

IV. NUMERICAL RESULTS

We present here the results of simulations made on BTW¹ and Zhang¹³ models. We have measured for these systems the critical energy and the average flow transferred from the boundaries at a generic scale k . Critical energy is defined as follows: we consider an external perturbation on a site in a coarse grained cell (k -cell) of size $l^{(k)} \times l^{(k)}$ and we look at the avalanches starting from this coarse-grained cell. If the avalanche transfers energy outside the given k -cell we compute the average energy $\varepsilon_c^{(k)}$ of that k -cell before the toppling; as a matter of fact, that k -cell is critical with a probability given by the frequency of the avalanches transferring energy outside the k -cell itself. Moreover, we define the energy transferred $\delta\varepsilon^{(k)}$ at the scale $l^{(k)}$ as the number of grains going outside the k -cell divided by the number of boundaries crossed and by the length $l^{(k)}$ (this is the trivial scaling).

If we look at numerical results (Fig. 6) we note that the critical energy at large scale is the average energy¹² of the system and this is not surprising since at the scale of the system size this is exactly what we compute. As for the behaviour of $\delta\varepsilon$ (Fig. 7) one gets that in the limit $k \rightarrow \infty$ it goes to zero. This result confirms the idea that the fixed point value for the rigidity is infinite, signalling a clear difference with respect to usual diffusive systems. The same qualitative results are obtained for the Zhang model¹³ (See Fig. 8 and 9).

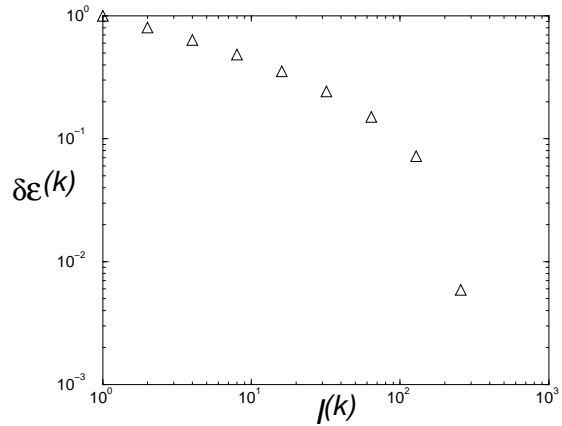


FIG. 7: Numerical renormalization of $\delta\varepsilon$ in the BTW.

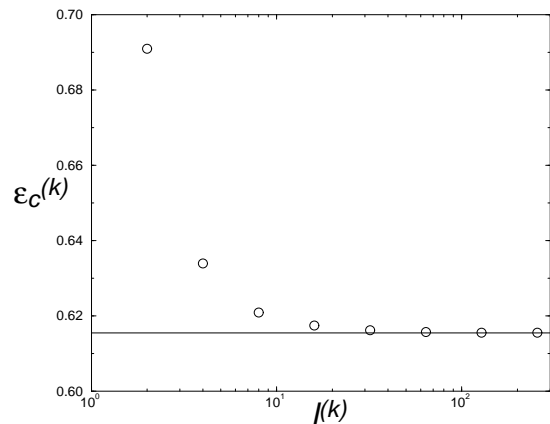


FIG. 8: The behaviour of the critical energy at a generic scale k for the Zhang model.

V. CONCLUSIONS

In summary we have investigated, both in the framework of the Dynamically Driven Renormalization Group scheme and by numerical simulations, the role of the so-called local rigidity in sandpile models. The local rigidity is defined as the ratio between the critical energy and the amplitude of the external perturbation, both at the microscopic scale. It turns out that, under the renormalization flow equations of the DDRG, the local rigidity renormalizes to an infinite fixed point value both for the BTW model and the Zhang model, while for a typical diffusive system one would expect a vanishing value. Numerical simulations of coarse-grained sandpile models confirm this picture.

Authors acknowledge EU contract FMRXCT980183 and G.C. acknowledge FET Open project COSIN IST-2001-33555.

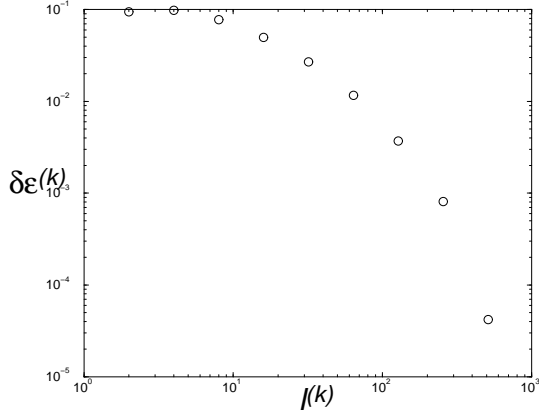


FIG. 9: Numerical renormalization of $\delta\varepsilon$ in the Zhang model.

VI. APPENDIX

• $\alpha = 3a$

In Fig. 10 we show all the possible paths starting from the perturbation of the critical site.

The probability relative to the first event at time t is the same as before, $\frac{1}{4}p_1 + \frac{1}{2}p_2 + \frac{3}{4}p_3 + p_4$. At time $t + 1$ we have a) $\frac{1}{4}p_1 + \frac{1}{6}p_2$ for the first two events in figure, $\frac{1}{6}p_2 + \frac{1}{4}p_3$ for the third (they are distinguishable only with respect to renormalization of $\delta\varepsilon$); b) $\frac{1}{6}p_2 + \frac{1}{4}p_3$ for the first two events, $\frac{1}{4}p_3 + p_4$ for the third; c) $\frac{1}{4}p_1 + \frac{1}{6}p_2$.

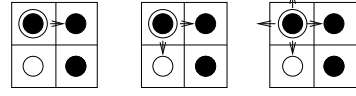
At time $t + 2$ we have $\frac{1}{4}p_1 + \frac{1}{3}p_2 + \frac{1}{4}p_3$ for the first two and $\frac{1}{6}p_2 + \frac{1}{2}p_3 + p_4$ for the third; in the renormalization of ε_c we have to consider only the sum $\frac{1}{2}p_1 + \frac{5}{6}p_2 + p_3 + p_4$. So we can write

$$\begin{aligned} \varepsilon_c^{(k+1)} = & \dots + w_{\alpha=3}^{(a)}(\rho) \cdot \langle \varepsilon_{\alpha=3}^{(k)} \rangle \cdot \left(\frac{1}{4}p_1 + \frac{1}{2}p_2 + \frac{3}{4}p_3 + p_4 \right) \times \\ & \times \left[\left(\frac{1}{2}p_1 + \frac{5}{6}p_2 + p_3 + p_4 \right) \left(1 + \left(\frac{1}{4}p_1 + \frac{1}{6}p_2 \right) \right) \right] + \dots \end{aligned} \quad (20)$$

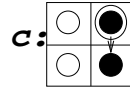
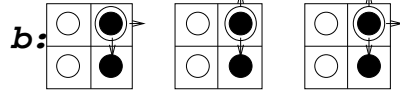
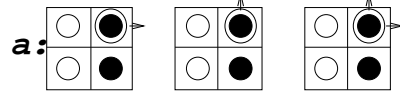
and

$$\begin{aligned} \frac{\delta\varepsilon^{(k+1)}}{\delta\varepsilon^{(k)}} = & \dots + w_{\alpha=3}^{(a)}(\rho) \cdot \left(\frac{1}{4}p_1 + \frac{1}{2}p_2 + \frac{3}{4}p_3 + p_4 \right) \times \\ & \times \left[\left(\frac{1}{2}p_1 + \frac{1}{2}p_2 + \frac{1}{4}p_3 \right) + \left(\frac{1}{6}p_2 + \frac{1}{4}p_3 \right) \times \right. \\ & \times \left. \left(\left(\frac{1}{4}p_1 + \frac{1}{3}p_2 + \frac{1}{4}p_3 \right) (2 + 1) + \left(\frac{1}{6}p_2 + \frac{1}{2}p_3 + p_4 \right) \frac{3}{2} \right) \right. \\ & \left. + \left(\frac{1}{6}p_2 + \frac{1}{4}p_3 \right) \left(\frac{1}{2}p_1 + \frac{5}{6}p_2 + p_3 + p_4 \right) + \left(\frac{1}{4}p_3 + p_4 \right) \right] \end{aligned}$$

$t :$



$t+1 :$



$t+2 :$

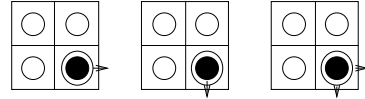


FIG. 10: Time t : the probability relative to the paths in figure is $\frac{1}{4}p_1 + \frac{1}{2}p_2 + \frac{3}{4}p_3 + p_4$.

$$\begin{aligned} & \left(\left(\frac{1}{4}p_1 + \frac{1}{3}p_2 + \frac{1}{4}p_3 \right) \left(\frac{3}{2} + 1 \right) + \left(\frac{1}{6}p_2 + \frac{1}{2}p_3 + p_4 \right) \frac{4}{3} \right) \times \\ & \times \left(\frac{1}{4}p_1 + \frac{1}{6}p_2 \right) \left(\frac{1}{2}p_1 + \frac{5}{6}p_2 + p_3 + p_4 \right) \Big] + \dots \end{aligned} \quad (21)$$

for the contributions coming from the $\alpha = 3a$ configuration.

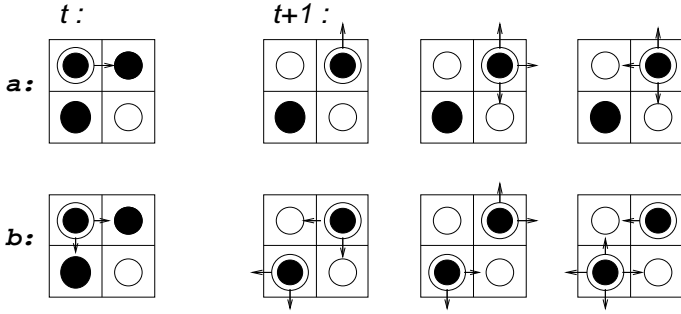
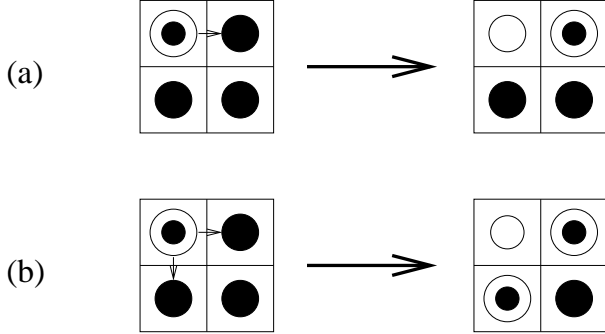
• $\alpha = 3b$

We can compute the probabilities of the shown in Fig. 11.

At time t we have to distinguish between two kinds of events: the toppling on a single site (this term is considered two times to include the toppling on the other site) and the one on two sites. The statistical weights are $\left(\frac{1}{4}p_1 + \frac{1}{3}p_2 + \frac{1}{4}p_3 \right)$ and $\left(\frac{1}{6}p_2 + \frac{1}{2}p_3 + p_4 \right)$ respectively. At time $t + 1$ both the events leave one flow going outside the cell, so we have:

$$\varepsilon_c^{(k+1)} = \dots + w_{\alpha=3}^{(b)}(\rho) \cdot \langle \varepsilon_{\alpha=3}^{(k)} \rangle \times$$

$$\times \left[2 \cdot \left(\frac{1}{4}p_1 + \frac{1}{2}p_2 + \frac{3}{4}p_3 + p_4 \right) \cdot \left(\frac{1}{2}p_1 + \frac{5}{6}p_2 + p_3 + p_4 \right) + \right.$$

FIG. 11: Evolutions for the $\alpha = 3b$ configuration.FIG. 12: Events a and b for the $\alpha = 4$ configuration.

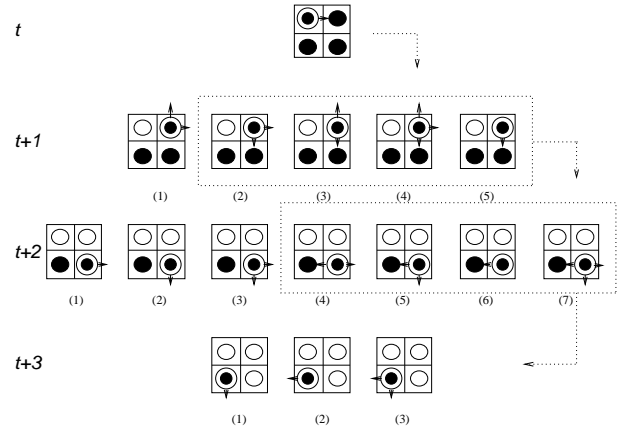
$$\begin{aligned}
 & + \left(\frac{1}{6}p_2 + \frac{1}{2}p_3 + p_4 \right) \cdot \left(1 - \left(\frac{1}{2}p_1 + \frac{5}{6}p_2 \right)^2 \right) + \dots \\
 & \frac{\delta \varepsilon^{(k+1)}}{\delta \varepsilon^{(k)}} = \dots + w_{\alpha=3}^{(b)}(\rho) \times \\
 & \times \left[2 \cdot \left(\frac{1}{4}p_1 + \frac{1}{2}p_2 + \frac{3}{4}p_3 + p_4 \right) \cdot \left(\frac{1}{2}p_1 + \frac{5}{6} + p_3 + p_4 \right) + \right. \\
 & \left. + \left(\frac{1}{6}p_2 + \frac{1}{2}p_3 + p_4 \right) \cdot \left(1 - \left(\frac{1}{2}p_1 + \frac{5}{6}p_2 \right)^2 \right) \right] + \dots \quad (23)
 \end{aligned}$$

• $\alpha = 4$

In a cell with all critical sites the number of possible time evolutions grows enormously. In Fig. 12 we show the first two possible events, with probabilities $p(a) = \frac{1}{4}p_1 + \frac{1}{3}p_2 + \frac{1}{4}p_3$ and $p(b) = \frac{1}{6}p_2 + \frac{1}{2}p_3 + p_4$. The paths coming from a are shown in Fig. 13 and the relative probabilities in Table I.

Now we have to compute 224 paths from the b event. The final result, avoiding details, for the renormalization of the critical height is

$$\begin{aligned}
 \varepsilon_c^{(k+1)} & = \dots + w_{\alpha=4}(\rho) \cdot \left\{ 2 \cdot \left(\frac{1}{4}p_1 + \frac{1}{3}p_2 + \frac{1}{4}p_3 \right) \times \right. \\
 & \times \left[\left(\frac{1}{2}p_1 + \frac{5}{6}p_2 + p_3 + p_4 \right) \cdot \left(1 + \left(\frac{1}{4}p_1 + \frac{1}{6}p_2 \right) + \right. \right.
 \end{aligned}$$

FIG. 13: Possible paths from event a .

	$t + 1$	$t + 2$	$t + 3$
(1)	$\frac{1}{2}p_1 + \frac{1}{2}p_2 + \frac{1}{4}p_3$	$\frac{1}{4}p_1 + \frac{1}{6}p_2$	$\frac{1}{4}p_1 + \frac{1}{3}p_2 + \frac{1}{4}p_3$
(2)	$\frac{1}{6}p_2 + \frac{1}{4}p_3$	$\frac{1}{4}p_1 + \frac{1}{6}p_2$	$\frac{1}{4}p_1 + \frac{1}{3}p_2 + \frac{1}{4}p_3$
(3)	$\frac{1}{6}p_2 + \frac{1}{4}p_3$	$\frac{1}{6}p_2 + \frac{1}{4}p_3$	$\frac{1}{6}p_2 + \frac{1}{2}p_3 + p_4$
(4)	$\frac{1}{4}p_3 + p_4$	$\frac{1}{6}p_2 + \frac{1}{4}p_3$	///
(5)	$\frac{1}{4}p_1 + \frac{1}{6}p_2$	$\frac{1}{6}p_2 + \frac{1}{4}p_3$	///
(6)	///	$\frac{1}{4}p_3 + p_4$	///
(7)	///	$\frac{1}{4}p_1 + \frac{1}{6}p_2$	///

TABLE I: Probabilities relative to the events in Fig. 13.

$$\begin{aligned}
 & + \left(\frac{1}{4}p_1 + \frac{1}{6}p_2 \right)^2 \left. \right] + \left(\frac{1}{6}p_2 + \frac{1}{2}p_3 + p_4 \right) \cdot \left[1 - \left(\frac{1}{4}p_1 \right)^2 + \right. \\
 & \left. - \left(\frac{1}{4}p_1 + \frac{1}{6}p_2 \right) \cdot \left(\frac{3}{4}p_1 + \frac{1}{6}p_2 \right) \cdot \left(\frac{1}{2}p_1 + \frac{1}{6}p_2 \right) \right] \left. \right\} \quad (24)
 \end{aligned}$$

If we introduce the quantities

$$\begin{aligned}
 \pi_1 & \equiv \frac{1}{4}p_1 + \frac{1}{2}p_2 + \frac{3}{4}p_3 + p_4 \\
 \pi_2 & \equiv \frac{1}{2}p_1 + \frac{5}{6}p_2 + p_3 + p_4 \\
 \pi_3 & \equiv \frac{1}{2}p_1 + \frac{1}{2}p_2 + \frac{1}{4}p_3 \\
 \pi_4 & \equiv \frac{1}{6}p_2 + \frac{1}{4}p_3 \\
 \pi_5 & \equiv \frac{1}{4}p_1 + \frac{1}{3}p_2 + \frac{1}{4}p_3 \\
 \pi_6 & \equiv \frac{1}{6}p_2 + \frac{1}{2}p_3 + p_4 \\
 \pi_7 & \equiv \frac{1}{4}p_1 + \frac{1}{6}p_2 \\
 \pi_8 & \equiv \frac{1}{2}p_1 + \frac{1}{6}p_2 \\
 \pi_9 & \equiv \frac{1}{4}p_3 + p_4 \\
 \pi_{10} & \equiv \frac{3}{4}p_1 + \frac{1}{2}p_2 + \frac{1}{4}p_3
 \end{aligned}$$

then we can write down the renormalization of $\delta\varepsilon$ as

$$\begin{aligned} \frac{\delta E^{(k+1)}}{\delta E^{(k)}} = & \dots + w_{\alpha=4}(\rho) \cdot \left\{ 2\pi_5 \left[\pi_3 + \right. \right. \\ & \pi_4 \left(2\pi_7 + \pi_4 \left(1 + \pi_2 + \frac{5}{2}\pi_5 + \frac{4}{3}\pi_6 \right) \right) + \\ & + \pi_9 \left(\frac{4}{3}\pi_5 + \frac{5}{4}\pi_6 \right) + \pi_7 \pi_2 + \pi_7 (2+1) + \\ & + \pi_4 \left(\frac{3}{2} + \left(\frac{3}{2} + \frac{3}{2} \right) \pi_5 + \pi_6 \right) + \pi_4 \left(\left(\frac{3}{2} + 1 \right) \pi_5 + \frac{4}{3}\pi_6 \right) + \\ & + \pi_9 \left(\left(2 + \frac{4}{3} \right) \pi_5 + \frac{5}{3}\pi_6 \right) + \pi_7 \pi_2 \left. \right\} + \pi_9 \times \\ & \times \left(\left(\frac{3}{2} + 1 \right) \pi_7 + \pi_4 \left(\frac{4}{3} + \frac{8}{3}\pi_5 + \frac{5}{4}\pi_6 \right) + \right. \\ & \left. \pi_4 \left(\frac{7}{3}\pi_5 + \frac{5}{4}\pi_6 \right) + \pi_9 \left(\left(\frac{5}{3} + \frac{5}{4} \right) \pi_5 + \frac{3}{2}\pi_6 \right) + \right. \\ & + \pi_7 \pi_2 \left. \right) + \pi_7 \left(\pi_3 + \pi_4 \left(\pi_2 + 3\pi_5 \frac{3}{2}\pi_6 \right) + \right. \\ & + \pi_9 \left(\frac{5}{2}\pi_5 + \frac{4}{3}\pi_6 \right) + \pi_7 \pi_2 \left. \right) \left. \right] + \pi_6 \times \\ & \left[\left(\pi_{10}^2 - \frac{1}{16}p_1^2 \right) + 2 \left(\pi_7 \pi_5 + \frac{1}{4}p_1 \pi_4 \right) \left(5\pi_5 + \frac{5}{2}\pi_6 \right) + \right. \\ & 2 \cdot \left(\pi_7 \pi_6 + \frac{1}{4}p_1 \pi_9 \right) \left(\frac{5}{2}\pi_5 + \frac{4}{3}\pi_6 \right) + \\ & + \left(2\pi_7 \pi_4 + \pi_4^2 \right) \left(10\pi_5 + \frac{17}{3}\pi_6 \right) + \left(2\pi_7 \frac{1}{4}p_1 + \pi_7^2 \right) \pi_2 + \\ & + 2 \left(\pi_4^2 + \pi_9 \pi_5 \right) \left(5\pi_5 + \frac{35}{12}\pi_6 \right) + \left(2\pi_9 \pi_4 + \pi_9^2 \right) \times \\ & \left. \left. \times \left(\frac{5}{2}\pi_5 + \frac{3}{2}\pi_6 \right) \right] \right\} \end{aligned} \quad (25)$$

¹ P. Bak, C. Tang, K. Wiesenfeld *Phys. Rev. Lett.* **4**, 381 (1987); *Phys. Rev. A* **38**, 364 (1988)

² H.J. Jensen, *Self-Organized Criticality*, Cambridge University Press (1998)

³ R. Dickman, M.A. Muñoz, A. Vespignani and S. Zapperi, *Paths to Self-Organized Criticality*, Short review in *Brazilian Journal of Physics*, **30**, 27 (2000) and references therein.

⁴ A. Vespignani, S. Zapperi *Phys. Rev. Lett.* **78**, 4793 (1997).

⁵ D. Sornette, A. Johansen, I. Dornic *J. Phys. I* (France) **5**, 325 (1995); A. Vespignani, S. Zapperi, V. Loreto *Phys. Rev. Lett.* **77**, 4560 (1996); *J. Stat. Phys.* **88**, 47 (1997)

⁶ M. Vergeles *Phys. Rev. Lett.* **75**, 1969 (1995)

⁷ A. Vespignani, S. Zapperi *Phys. Rev. E* **57**, 6345 (1998), A. Gabrielli, G. Caldarelli, L. Pietronero *Phys. Rev. E* **62**,

7638 (2000)

⁸ R. Caferio, V. Loreto, L. Pietronero, A. Vespignani, S. Zapperi *Europhys. Lett.* **29**, 111 (1994)

⁹ L. Pietronero, A. Vespignani, S. Zapperi *Phys. Rev. Lett.* **72**, 1690 (1994); A. Vespignani, S. Zapperi, L. Pietronero *Phys. Rev. E* **51** 1711 (1995)

¹⁰ A. Vespignani, S. Zapperi and V. Loreto, *Phys. Rev. Lett.* **77**, 4560 (1996); A. Vespignani, S. Zapperi and V. Loreto, *J. of Stat. Phys.* **88**, 47 (1997).

¹¹ L. Pietronero, P. Tartaglia, Y.-C. Zhang *Physica A* **173**, 129 (1991)

¹² V.B. Priezzhev *J. Stat. Phys.* **74**, 955 (1994)

¹³ Y.-C. Zhang *Phys. Rev. Lett.* **63**, 470 (1989)